Rates of active faulting during late Quaternary fluvial terrace formation at Saxton River, Awatere fault, New Zealand

Dougal P.M. Mason[†]
Timothy A. Little[‡]
School of Earth Sciences, Victoria University, P.O. Box 600, Wellington, New Zealand

Russ J. Van Dissen[§]
Institute of Geological and Nuclear Sciences Ltd., P.O. Box 30368, Lower Hutt, New Zealand

ABSTRACT

A flight of faulted fluvial terraces at Saxton River on the Awatere fault, northeast South Island, New Zealand, preserves the incremental slip history and detailed paleoearthquake chronology of this major strike-slip fault. Here, six fluvial terraces have been progressively displaced across the inland Molesworth section of the fault, with horizontal displacements ranging from ~6 m for an ephemeral channel on the youngest terrace to 81 m for the riser above the oldest terrace. New optically stimulated luminescence ages for abandonment of the two oldest terrace treads are 14.5 ± 1.5 and 6.7 ± 0.7 ka. When combined with new measurements of incremental horizontal displacements and previous age data, these new ages indicate that strike-slip on this part of the Awatere fault has been occurring at a near-constant rate of 5.6 ± 0.8 mm/yr since ca. 15 ka. This rate is similar to recent slip-rate estimates for an adjoining section of the same fault to the east, which suggests that there is near-complete slip transfer across the junction between the two fault strands. Comparison of the magnitudes and ages of the terrace riser displacements to the timing of paleoearthquakes on the Molesworth section allows the mean per event horizontal displacement over the eight most recent surface-rupture events to be estimated at 4.4 ± 0.8 m. Between ca. 5 ka and ca. 2 ka, surface-rupturing earthquakes increased in frequency and decreased in their mean coseismic displacements to <2.6 m. During this time, the sense of local dip slip also shifted from north-side-up to south-side-up. Rapid incision of Saxton River in the mid-Holocene may have caused a perturbation in the near-surface stress directions acting on the fault plane beneath the Saxton River valley, forcing a change in the near-surface fault geometry that resulted in the shift in sense of dip slip.

Keywords: coseismic processes, neotectonics, paleoseismicity, river terraces, slip rates, strike-slip faults.

INTRODUCTION

Flights of fluvial terraces are valuable geomorphic markers for preserving the progressive slip history of faults. Flights of faulted terraces preserve both horizontal and vertical components of slip, commonly across thousand-year time scales, which may be used to examine the constancy or variation of the rates and kinematics of fault slip through time. It is not common, however, for incremental terrace displacements on a strike-slip fault to be related directly to a detailed paleoearthquake history at the same site.

In this study, we integrate new terrace abandonment ages and fault displacement data with a detailed chronology of surface-rupturing paleoearthquakes from a flight of well-preserved faulted fluvial terraces on the eastern bank of Saxton River on the Awatere strike-slip fault, in New Zealand (Fig. 1). These data are used to evaluate the variation in the rates of strike-slip and kinematics of surface-rupturing paleoearthquakes over the last ~15 k.y. on a major active strike-slip fault in the Marlborough fault system in South Island, New Zealand.

In Marlborough, relative motion between the Pacific and Australian plates is ~39 mm/yr at a mean azimuth of ~253° (De Mets et al., 1990, 1994; Fig. 1). This relative motion is accommodated across a zone of active strike-slip faults (the Marlborough fault system), which links the Alpine fault transform plate boundary to the south with the westward-directed Hikurangi subduction margin to the north (Lewis and Pettinga, 1993; Walcott, 1998). Knuepfer (1992) presented ages, displacements, and rates of slip for faulted geomorphic surfaces at 16 sites across the Marlborough fault system, including the Saxton River terraces on the Awatere fault, and interpreted the results as revealing distinct temporal and spatial variations in late Quaternary slip across this zone of transcurrent faulting. His data suggested a dramatic decrease in lateral slip rate in the last 3–5 k.y., which was interpreted to be a manifestation of short-term (i.e., 10^3 yr) changes in convergence accommodated across this part of the plate boundary zone. If correct, such a dramatic variation in fault slip rates would have important implications regarding the temporal variability of earthquake hazard along those active faults, as well as the tempo and nature of plate boundary processes in active deformation zones such as those in the South Island of New Zealand.

The Awatere fault is one of four principal strike-slip faults in the Marlborough fault system, and is composed of two geometrically defined fault sections (the eastern and Molesworth sections, Fig. 1B). These intersect at a conspicuous junction near the Molesworth Station homestead in the upper Awatere Valley. Eighteen kilometers to the west of this junction, the Molesworth section of the fault lies at the northern margin of a sedimentary basin that has been infilled with Quaternary alluvium deposited by the Saxton and Acheron Rivers (Fig. 1C). On the eastern side of Saxton River, late Pleistocene aggradational fans have been eroded into a flight of well-preserved fluvial terraces that have been displaced by the fault (Fig. 2). These terraces have provided key slip data for this and previous studies of the Awatere fault (e.g., Wellman,

[†]Present address: Opus International Consultants Ltd., P.O. Box 12-003, Wellington, New Zealand; Dougal.Mason@opus.co.nz.
[‡]E-mail: Timothy.Little@vuw.ac.nz.
[§]E-mail: r.vandissen@gns.cri.nz.

GSA Bulletin; November/December 2006; v. 118; no. 11/12; p. 1431–1446; doi: 10.1130/B25961.1; 13 figures; 4 tables; Data Repository item 2006193.

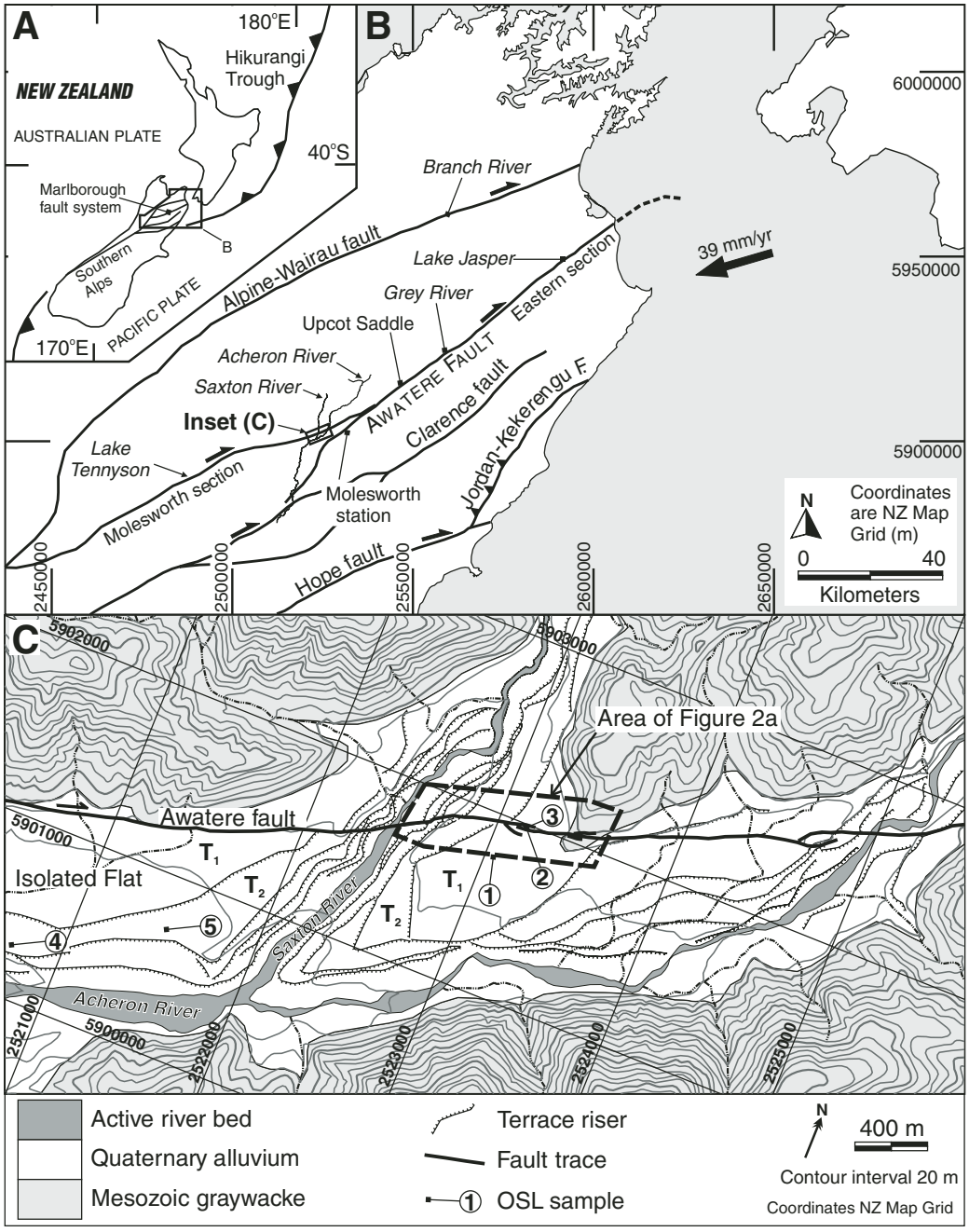

Figure 1. (A) The Pacific-Australia plate boundary through New Zealand. (B) The Marlborough fault system. The principal active faults are shown, along with key locations mentioned in the text (after Carter et al., 1988; Little and Roberts, 1997; Nicol and Van Dissen, 2002). Half arrows on the principal faults and barbs on the Jordan thrust indicate the sense of motion. The bold arrow indicates the azimuth (with the magnitude stated alongside) of Pacific plate motion relative to the Australian plate (De Mets et al., 1990, 1994). (C) The Awatere fault trace at Isolated Flat. Quaternary alluvium deposited by the Saxton and Acheron Rivers has been cut into a series of terraces since the late Pleistocene, which subsequently have been displaced by the Awatere fault. The T_1 and T_2 treads are labeled. The locations of new optically stimulated luminescence (OSL) samples (circled locations 1–5) and the area of Figure 2 are also shown.

1953; Lensen, 1973; Knuepfer, 1992; McCalpin, 1996a).

We have remeasured the terrace displacements using microtopographical maps constructed from centimeter-precision global positioning system (GPS) surveys and dated the two oldest terraces by optically stimulated luminescence (OSL) dating. These new data refine the incremental and long-term rates of dextral strike-slip over the last 15 k.y. on the Molesworth section of the Awatere fault. In addition, a new paleoearthquake chronology has been developed from a trench excavated into the oldest terrace at Saxton River (Mason et al., 2004), which allows incremented terrace displacements to be attributed to one or more surface-rupturing paleoearthquakes dated by ^{14}C. The Saxton River terraces therefore provide important data from which we can: (1) evaluate slip-rate constancy or variation across a time span of ~15 k.y., (2) assess the efficiency of slip transfer across a major junction between two strike-slip fault strands, (3) relate incremental terrace offsets to a known earthquake chronology, thereby assessing the consistency, or otherwise, of single-event surface-rupture displacements through time, and (4) reconstruct the late Quaternary incision history of Saxton River.

SUMMARY OF PRINCIPLES, TERMINOLOGY, AND METHODS

In this study, Lensen's (1964a, 1968, 1973) nomenclature for terraces is adopted. A terrace "tread" is defined as the near-horizontal top surface of each unit of fluvially deposited terrace gravel (originally the river bed), and the "riser" is the sloping erosional surface that links one terrace level to the next (originally the riverbank).

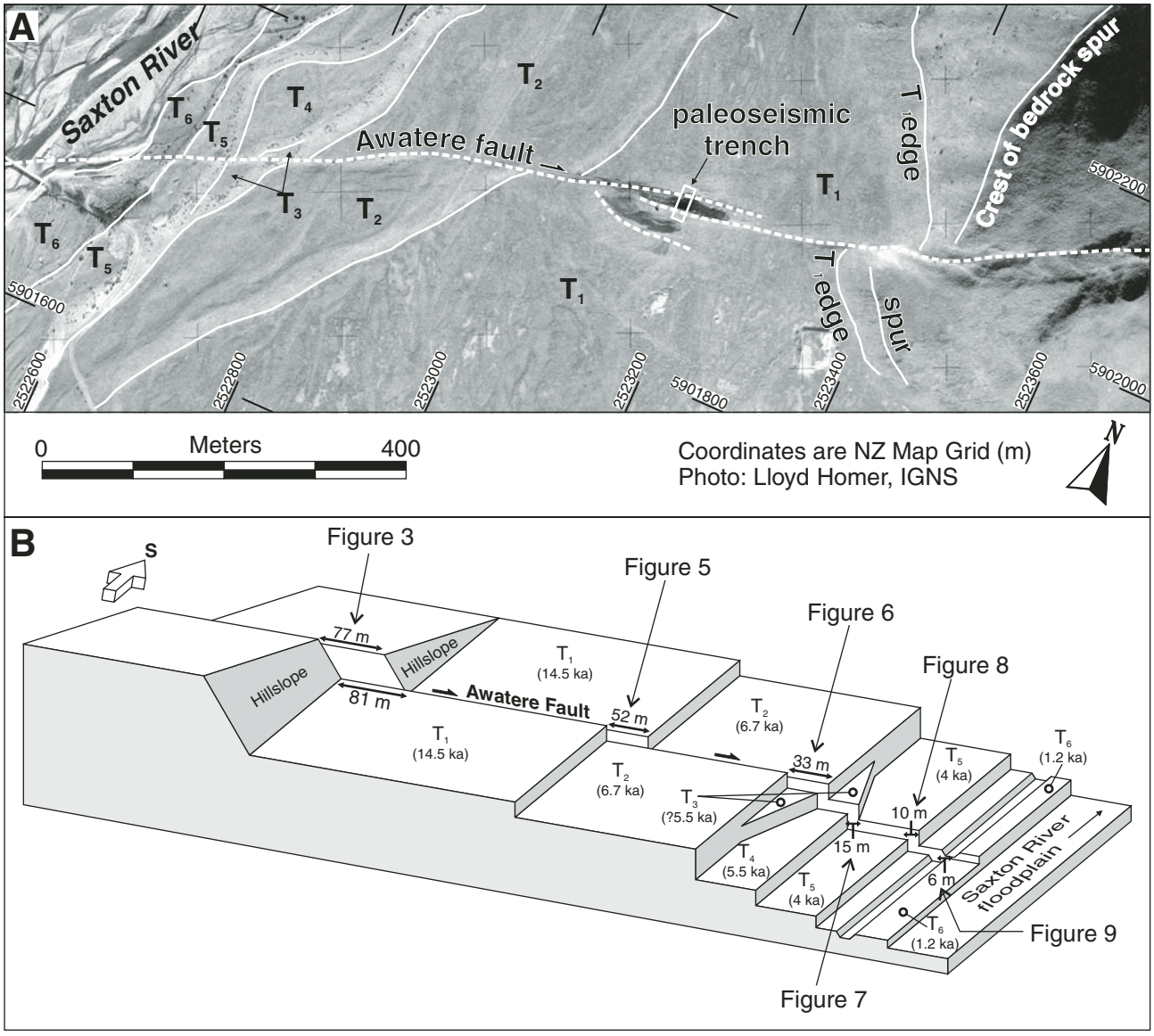

Figure 2. (A) Aerial photo of the eastern bank of Saxton River and the terraces mapped in this study. The crests of the terrace risers and other relevant geomorphic features have been accentuated with white lines, and the location of a paleoseismic trench (Mason et al., 2004) is also shown. (B) Vertically exaggerated block diagram looking south across the Saxton River terraces, with the preferred tread ages and horizontal offsets of terrace risers labeled (see Tables 1 and 2 for the bracketing uncertainties of these measurements). IGNS—Institute of Geological and Nuclear Sciences.

We refer to the oldest terrace as T_1, with younger surfaces numbered upward. All the terraces on the east bank of Saxton River were surveyed using a Leica Real-Time Kinematic (RTK) GPS system with points on the ground surface sampled every 2 m. The raw GPS data were processed into New Zealand Map Grid coordinates, gridded with a grid spacing of 0.5 m, and contoured using the terrain modeling program Surfer v.8 (Golden Software Inc.). Microtopographical maps of individual terrace offsets were created to allow detailed measurement of the displacements.

Terrace displacements were measured using the linear projection method described in Little et al. (1998). This method is especially appropriate where risers have dissimilar heights across a fault as a result of vertical fault displacements taking place when the river still occupied the lower terrace (at Saxton River, riser heights commonly differ by up to 1 m across the fault). The method assumes that the river was able to trim its banks efficiently up until a terrace was abandoned. Riser displacements are inferred to accumulate after the river's abandonment of the lower terrace surface (see following). Thus, it is the toe, rather than the crest of each riser that is the key linear reference marker for measuring fault slip. Also, the terrace risers at Saxton River are not vertical, but have been modified by erosion at the top of the riser and deposition at their base. For these reasons, we selected an arbitrary linear marker (topographical contour) near the mid-point of each displaced riser. This contour, although arbitrary, is uniquely identifiable on both sides of the fault by its fixed elevation above the lower terrace surface. There is no "error" associated with this choice of reference contour, as these are arbitrarily chosen.

TABLE 1. MEASUREMENTS OF HORIZONTAL OFFSETS OF THE SAXTON RIVER TERRACES, FROM THIS AND PREVIOUS STUDIES. MEASUREMENTS OF VERTICAL TERRACE OFFSETS, TREAD WIDTH DIFFERENCES, RISER HEIGHT DIFFERENCES, AND THE HEIGHTS OF THE TERRACE TREADS ABOVE THE MODERN RIVER ARE ALSO LISTED

Terrace feature	Horizontal offset (m)					Vertical offset [this study] (m)†	Tread width difference (m)‡	Riser height difference (m)§	Tread height above river (m)
	This study		Lensen (1973)	Knuepfer (1992)	McCalpin (1996a)				
Hillslope	77	±15	72	66 ± 5	60–64	2.6 ± 1.6			
T_1 edge	81	±21							
T_1 tread						3.0 ± 1.8	–91.8		19.9
T_1-T_2 riser	52	+6 –12	72	52 ± 5	62–70			–0.5	
T_2 tread						1.9 ± 0.2	26.5		17.3
T_2-T_3 riser	33	+3 –4	37	35 ± 5	35.2–42			–0.2	
T_3 tread						0.7 ± 0.2	–9.3		11.1
T_3-T_4 riser	15	+0.5 –2.1	15	15 ± 4	11.5–12.0			6.4	
T_4 tread									9.5
T_5 tread						–0.5 ± 0.2	11.9		4.7
T_5-T_6 riser	10	+0.5 –2	7.6	8 ± 2	7.2–7.6			–1.3	
T_6 tread	6.3	±0.8	6.7	7.2 ± 0.5	7.2–7.6	–0.4 ± 0.1	1.1	0.4	1.9

†A negative value indicates the sense of throw is up to the south.
‡Calculated by subtracting the width of the tread on the south side of the fault from the tread width on the north side.
§Calculated by subtracting the height of the riser on the south side of the fault from the riser height on the north side.

The advantage of choosing a mid-slope contour, approximately halfway down the riser on one side of the fault is that this is the only part of the original riser slope that may have remained unmodified by any erosion or deposition (unlike the current crest or toe). Because of vertical offset on the fault subsequent to riser formation, the faulted equivalents of this originally continuous reference contour today lie at different elevations on opposite sides of the fault. This inferred vertical mismatch is the same as the difference in elevation of the lower terrace treads on either side of the fault. Measuring this throw allows the faulted position of this arbitrary (mid-slope) reference contour to be matched on the opposite side of the fault from where it was first defined. Projections of the maximum and minimum offsets are made so the trend is the same on each side of the fault. This method assumes that prior to slip and erosion on the fault scarp, each riser segment in close proximity to the scarp had a common trend at the fault. We did not measure displacements by graphical matching of equivalent fault-parallel profiles (e.g., McCalpin, 1996b) because (1) the offset risers were generally not perpendicular to the fault; and (2) erosionally unmodified profiles immediately adjacent to the fault on both sides were not available, thus this technique would have required an additional projection procedure very similar to the one we used.

Calculating rates of fault displacement requires interpretations of the age at which these landforms began to preserve fault slip. At Saxton River, the modern river is actively trimming the T_6 riser (the modern river bank), removing any pre-existing fault displacement that may have offset the present river bank during the last earthquake. Knuepfer (1992) made a similar inference about effective river-bank trimming throughout the Marlborough fault system where other rivers are traversed by active faults. Another observation in support of effective riser trimming is the difference in the fault-parallel width of the T_2 tread across the fault (26.5 m, a measure of syn-T_2 displacement for a case of efficient riser trimming; see Table 1). This difference is approximately equivalent to the horizontal offset between the T_1-T_2 and T_2-T_3 risers (19 m, another independent measure of syn-T_2 slip; see Table 1; Fig. 2B). This suggests that the T_2-T_3 riser was completely trimmed ("zeroed") during downcutting to T_3 (see Lensen, 1964a). Displacement of the T_2-T_3 riser is therefore assumed to have begun to accumulate following abandonment of T_3, and the age of T_3 abandonment thus provides a (minimum) age for the total offset of the T_2-T_3 riser. This relationship forms the basis for all our slip-rate calculations: horizontal displacement of a terrace riser is dated by the age of the tread immediately below that riser. If incorrect, this assumption will yield a maximum slip-rate estimate, because incomplete trimming prior to abandonment of the lower surface means that some of the observed riser offset would have been "inherited" from the previous riverbank geometry.

FAULT DISPLACEMENT DATA

Wellman (1953) mapped four fluvial terraces on the eastern side of Saxton River by aerial photograph analysis, identifying progressively increasing vertical and horizontal offsets of older terrace risers and tread heights above the modern river level, and inferring a local fault strike of 067°. Lensen (1973) surveyed the Saxton River area with a measuring tape, stadia rod, and theodolite, and mapped five terrace surfaces. He documented fault displacements of the terrace risers and treads (see Table 1), assumed a late-glacial age of ca. 18 ka for the highest terrace, and interpreted a near-uniform rate of horizontal faulting since that time. Knuepfer (1992) presented new ages for the five terraces as mapped by Lensen, based on calibrating pebble weathering rind thickness measurements to rind-growth curves calculated from surfaces with numerical ages (e.g., ^{14}C-based ages, see Knuepfer, 1988). Knuepfer's data suggested a prominent decrease in lateral slip rate at ca. 4 ka, from 9.4 mm/yr in the early Holocene to 3.8 mm/yr in the late Holocene. McCalpin (1996a) remeasured the fault displacements, presented a new ^{14}C-based age for the youngest terrace, and attributed displacement of this terrace to coseismic slip during only the most recent surface-rupturing event.

We mapped six terraces at Saxton River, which is a revision of the five surfaces mapped by Lensen (1973), Knuepfer (1988, 1992) and McCalpin (1996a). Our addition of a terrace was due to detailed aerial photoanalysis and

GPS-based surface modeling of the terraces, which allowed differentiation of an extra terrace level (here called T_4) in what previous workers considered a single surface (T_3 of Lensen, 1973; see Figures 3A and 3B). Our GPS mapping shows that T_4 has been completely removed on the south side of the fault, near the fault scarp as a result of lateral erosion when the river occupied T_5.

The flight of terraces at Saxton River shows progressively increasing fault displacement with increasing surface height and relative age (Fig. 2B; Table 1). Seven displacements were measured at Saxton River: one of a bedrock spur to the east of (and above) the highest (T_1) terrace surface, one of the eastern edge of T_1, four of terrace risers (T_1-T_2, T_2-T_3, T_4-T_5, and T_5-T_6), and one of an abandoned channel incised into the T_6 surface. We measured horizontal and vertical offsets of the terraces and their risers, and the heights of each terrace tread above the modern river level. These measurements are compiled in Table 1, along with previous measurements of terrace offsets at Saxton River. Below the T_6 surface is the active Saxton River floodplain, and therefore the "T_6 riser" is the modern riverbank. As mentioned already, this does not preserve any fault displacement.

The two largest measured horizontal displacements are those of the displaced crest of the bedrock spur and the eastern edge (referred to as the back edge) of T_1, which flanks that spur. The spur has been offset horizontally by 77 ± 15 m (Fig. 4A). The vertical offset of the hillslope is not well constrained because erosion and tectonic deformation have resulted in a zone of slumping and bulging adjacent to the fault scarp. To estimate the vertical offset of the hillslope, fault-perpendicular profiles of the hillslope were constructed and projected to the fault beneath the mantle of slope colluvium near the fault (Fig. 4C). The separation of the projected hillslope profiles across the fault indicates a vertical offset of 2.6 ± 1.6 m (north side upthrown).

The nearby T_1 back edge has been offset horizontally by 81 ± 21 m and vertically by 3.0 ± 1.8 m, with the north side upthrown (Fig. 4A). The horizontal slip was estimated by measuring the offset between projected terrace edges at the fault scarp, and this yielded 60–102 m of inferred slip, depending on the inferred trend of that edge in the vicinity of the fault. We used the mean of these values as our estimate of strike-slip offset, to which we assigned a symmetrical uncertainty of ±21 m. The position of the terrace edge on the north side of the fault was not assumed to coincide with the present-day slope break between the hillslope and the terrace tread, but was instead based on fault-subparallel profiles of the terrace surface that were projected to intersect the steep flank of the adjacent bedrock hillslope (see Fig. 4B). These profiles intersect one another beneath an apron of hillslope-derived colluvium, defining the present-day slope break. A larger offset (up to 65%) is obtained using this buried position of the terrace edge than by projecting the topographic slope break to the fault scarp (~60 m).

Our GPS-based data indicate that the T_1-T_2 riser is dextrally offset by 52 (+6, −12) m (Fig. 5). Lensen (1973) measured this displacement to be 72 m (Table 1). The difference between our measurement and Lensen's is most likely due to interpretations of the original curvature of the riser. We assumed that the curvature of this riser derives from the original meandering or braided geometry of the riverbanks. Projection of the terrace riser to the fault trace was therefore made along the curved trend of the riser, resulting in a smaller horizontal separation measurement than that of Lensen, who assumed a near-linear terrace edge and that this edge intersected the fault at a 70° angle. This difference in inferred projection geometry is shown in Figure 5, with projection N3 being that of Lensen (1973), whereas projections S1-N2 and S2-N1 represent the range of (curved) terrace edge geometries employed in our smaller estimate. Measurement of the offset of the T_1-T_2 riser is slightly complicated by splaying and bifurcation of the fault trace at the intersection of the terrace risers with the fault trace, resulting in the development of a 30–50-m-wide transtensional pull-apart depression on the T_1 tread. The opening of this pull-apart appears to have separated the piercing points of this riser along an ~NNE-SSW trend away from the main fault scarp (Fig. 5).

Vertical offset of the T_2 tread below this riser was measured to be 1.9 ± 0.2 m, upthrown to the north. The T_1 tread is upthrown by a similar amount <200 m to the east, although right-stepping, bifurcating fault strands on this tread have formed two ~50-m-long sag ponds in the downthrown graben between the fault scarps, and therefore the net vertical offset of T_1 may be negligible.

The T_2-T_3 riser has been horizontally offset by 33 (+3, –4) m (Fig. 6), which is similar to the previous measurements of 35–37 m made by Lensen (1973), Knuepfer (1992), and McCalpin (1996a). The T_3 tread adjacent to this riser is vertically offset by 0.7 ± 0.2 m, with the north side upthrown. On the T_2 tread 50 m to the east of this riser, a 1–2-m-high, 60–80-m-long pressure ridge has formed on the south side of the fault adjacent to a 5–10° anticlockwise change in the strike of the fault (restraining bend). While formation of this bulge has resulted in localized uplift of the T_2 tread on the southern side of the fault, 140 m farther to the east, below the T_1-T_2 riser, the T_2 tread is upthrown to the north, which is consistent with the sense of throw of the T_3 tread across the fault.

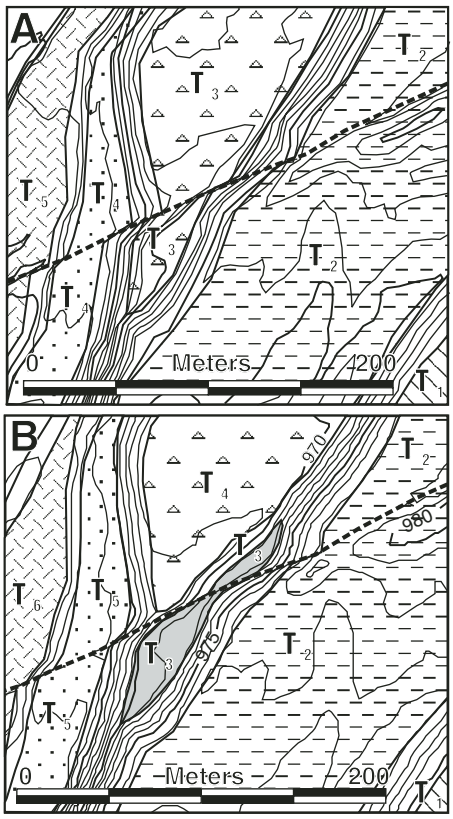

Figure 3. (A) Enlargement of T_3 as mapped by New Zealand Aerial Mapping in 1969 and by Lensen (1973). (B) Enlargement of the same area as A, showing our differentiation of an additional terrace, here called T_4.

T_3 is only preserved as small terrace remnants adjacent to the fault scarp. Lensen (1973), Knuepfer (1992), and McCalpin (1996a) all measured horizontal offsets of 12–15 m of a riser immediately below their T_3. Based on field observations, low-altitude aerial photographs, and GPS survey data, we subdivided this tread (their T_3) into two levels (our T_3 and T_4), as shown in Figures 7 and 8. T_4 has apparently been trimmed on the south side of the fault, where it has been completely removed. Both the T_4 (locally completely removed) and T_3 treads were trimmed against a terrace riser that was cut during occupation of the T_5 tread (Fig. 7). This riser has been dextrally offset by 15 (+0.5, –2.1) m.

The T_5-T_6 riser is offset along the fault by 10 (+0.5, –2) m dextrally and 0.5 ± 0.2 m vertically, with the south side upthrown (Fig. 8). An abandoned channel incised into the T_6 surface records the smallest measured displacement at the Saxton River locality as was first recognized by Lensen (1973). His measurement of 6.7 m

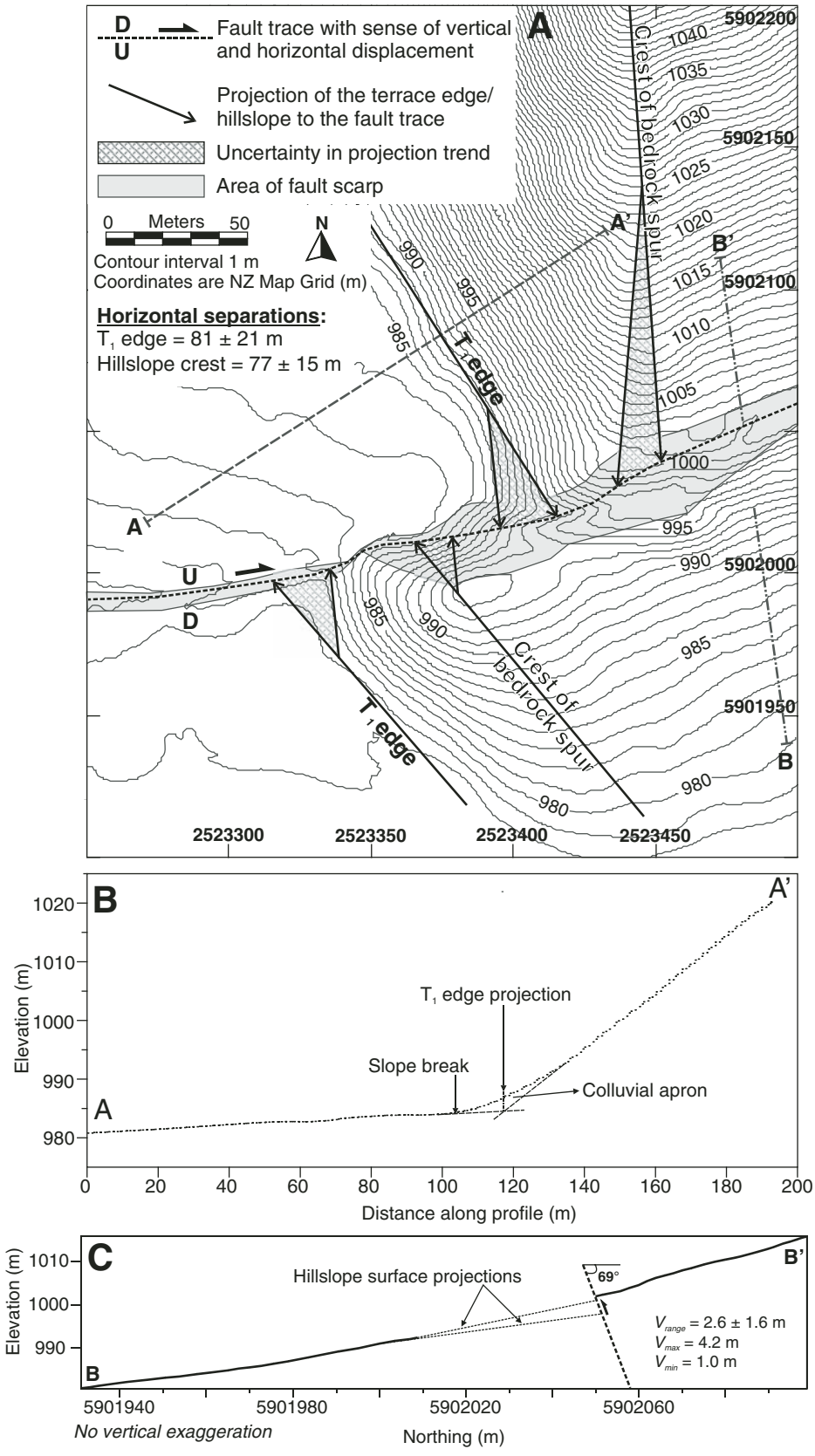

Figure 4. (A) Map of the hillslope and T_1 edge offsets. The profile B-B′ is shown in Figure 5. (B) Profile across the T_1 tread and adjacent hillslope, showing our projected position of the T_1 edge. (C) Fault-perpendicular profiles used to estimate vertical offset of the hillslope. The hillslope surface was projected upslope to the fault plane to estimate the maximum and minimum vertical offsets. The fault dip at this site was estimated by constructing structural contours on the fault trace across the hillslope.

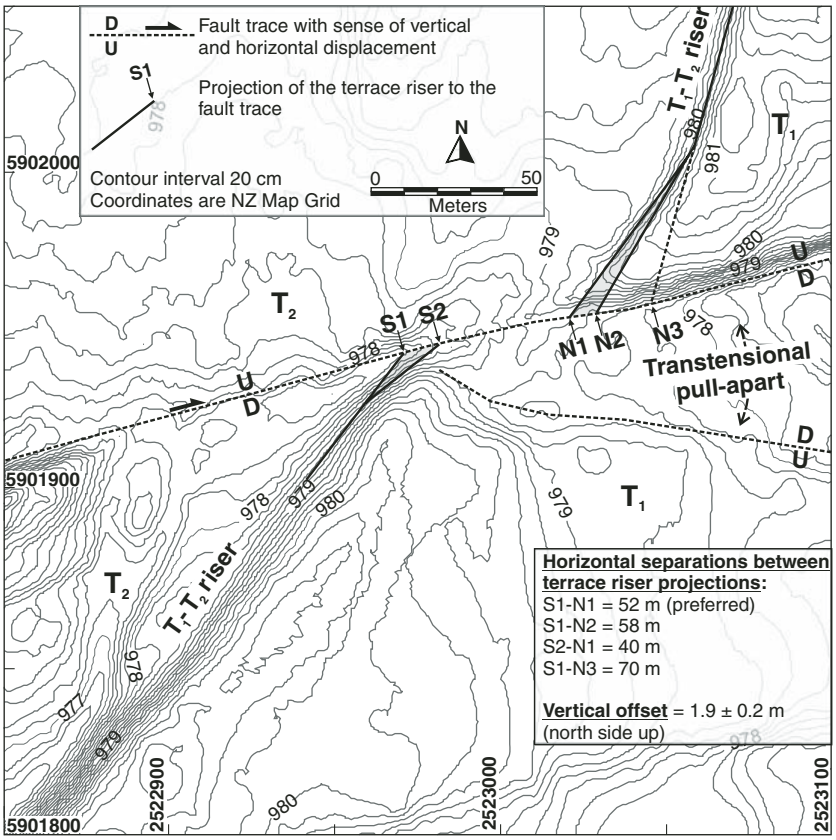

Figure 5. Map of the T_1-T_2 riser offset. The projection "N3" represents a near-linear terrace edge projection (such as that of Lensen, 1973), whereas projections N1 and N2 represent originally curved terrace edge projections.

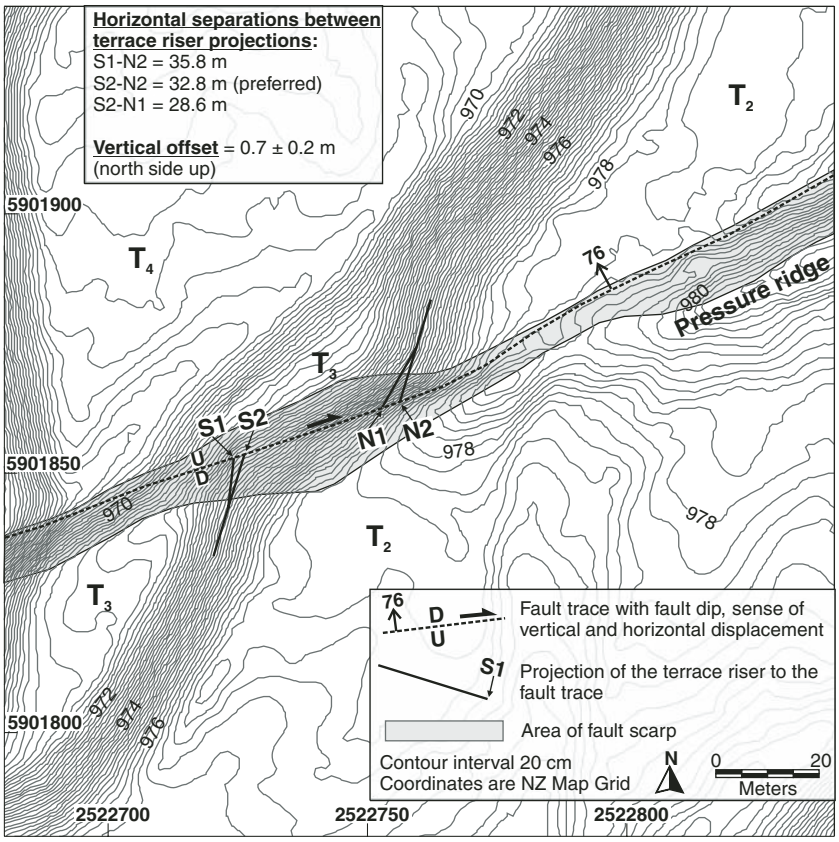

Figure 6. Map of the T_2-T_3 riser offset.

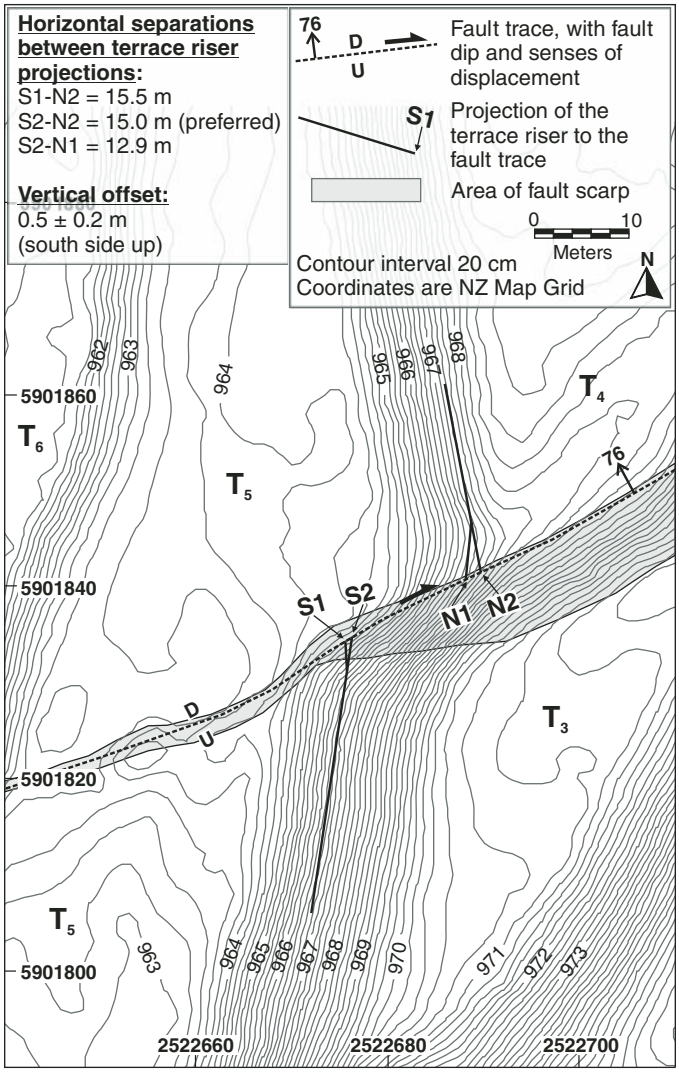

Figure 7. Map of the offset riser above the T_5 tread and below the T_3 and T_4 treads.

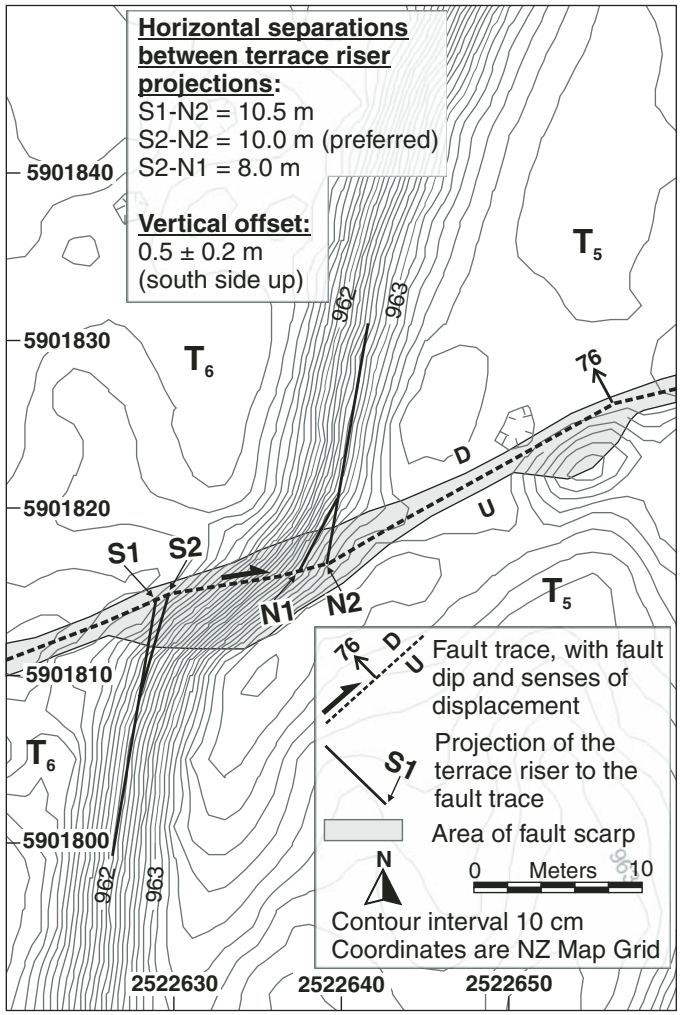

Figure 8. Map of the T_5-T_6 riser offset.

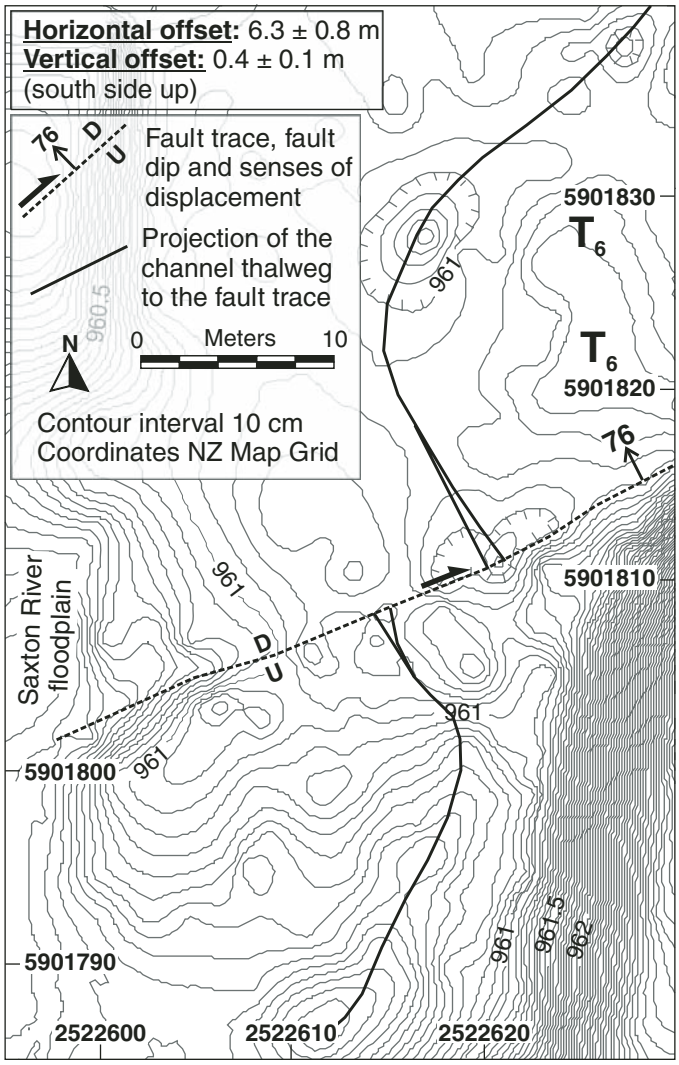

Figure 9. Map of the offset channel on the T_6 tread.

(Table 1) is probably the most reliable available, as this channel was subsequently modified by excavation along the fault scarp to enhance drainage of this terrace and is no longer an obvious geomorphic feature. Nevertheless, we were able to differentiate this channel on the microtopographic map of the T_6 tread, and allowing projection of the remnant channel thalwegs to the fault (Fig. 9), the GPS data yielded a horizontal offset for this channel of 6.3 ± 0.8 m, and a south-side-up vertical offset of the T_6 surface of 0.4 ± 0.1 m.

TERRACE ABANDONMENT AGES

All previous estimates of terrace abandonment ages at Saxton River are listed in Table 2. Knuepfer (1988) presented ages for the Saxton River terraces based on modal thicknesses of weathering rinds developed on Torlesse sandstone cobbles on the terrace surfaces, calibrated to established rind-growth curves (e.g., Chinn, 1981; McSaveney, 1992). The accuracy of ages obtained using this method was stated by Knuepfer (1988) to be ±5% to ±40%. Using the optically stimulated luminescence (OSL) dating technique, we dated five samples; one from the tread of T_1 (OSL-1), two from the tread of T_2 (OSL-4, OSL-5), and two from a paleoseismic trench (Saxton trench; Mason et al., 2004) excavated across a sag pond on T_1 (OSL-2, OSL-3). The samples were dated at the Victoria University of Wellington (VUW) luminescence laboratory, and the dating results are summarized in Table 3. Stratigraphic columns and/or detailed trench logs for each of these five OSL samples are provided in the GSA Data Repository (See Figs. DR-1, DR-2, DR-3, DR-4; and Table DR-1).[1] In addition, twelve ^{14}C ages were determined for sediments deposited on the T_1 surface as exposed in the walls of the Saxton paleoseismic trench (for these locations and results, see Figs. DR-2, DR-5, and DR-6, and Tables DR-1 and DR-2). In the Saxton trench, the two OSL samples (OSL-2, OSL-3) and 12 radiocarbon ages together provide a detailed and internally consistent chronology of deposition postdating the abandonment of T_1.

TABLE 2. PREVIOUS TERRACE TREAD AGE ESTIMATES AT SAXTON RIVER

Terrace feature	Pebble weathering rind calibration (ka)†	^{14}C dating of carbon within fluvial silts (cal. k.y. BP)‡
T_1 tread	9.41 ± 1.57	
T_2 tread	7.15 ± 1.1	
T_3 tread	>5.46 ± 0.77	
T_4 tread	5.46 ± 0.77	
T_5 tread	4.0 ± 1.0	
T_6 tread	2.0 ± 0.5	1.17 ± 0.11

†Knuepfer (1992).
‡McCalpin (1996a).

For the OSL samples, deposition ages were determined for all samples using the silt (4–11 μm) fraction of feldspar. The paleodose, i.e., the radiation dose accumulated in the sample after the last light exposure (assumed at deposition), was determined by measuring the blue luminescence output during infrared optical stimulation (which selectively stimulates the feldspar fraction). The dose rate was estimated on the basis of low-level gamma spectrometry. The paleodoses were estimated by use of the multiple aliquot additive-dose method (with late-light subtraction). The samples were counted using high-resolution gamma spectrometry with a broad energy Ge detector for a minimum time of 24 h. The spectra were analyzed using GENIE2000 software. The dose-rate calculation was based on the activity concentration of the nuclides ^{40}K, ^{208}Tl, ^{212}Pb, ^{228}Ac, ^{214}Bi, ^{214}Pb, and ^{226}Ra.

The three OSL samples taken from the T_1 and T_2 treads (OSL-1, OSL-4, and OSL-5) were taken 20 cm above the base of sandy silt that mantles the gravel alluvium. The sampled sediment accumulations on the terrace treads are lobate, anastomosing lenses of sandy silt <1 m thick. These may well be remnant interfluves between gravel-based meander channels that were deposited as overbank levees and crevasse channel fans when the terraces were last occupied (e.g., Miall, 1992). The OSL ages are

[1]GSA Data Repository item 2006193, containing details of OSL dating methodology, as well as stratigraphic columns and fault trench logs for the dated OSL and radiocarbon samples, is available on the Web at http://www.geosociety.org/pubs/ft2006.htm. Requests may also be sent to editing@geosociety.org.

TABLE 3. RESULTS OF OPTICALLY STIMULATED LUMINESCENCE (OSL) DATING OF SILT FROM SAXTON RIVER TERRACES

	Sample number				
	OSL-1	OSL-2	OSL-3	OSL-4	OSL-5
Lab No.	WLL179†	WLL360‡	WLL501	WLL500	WLL180†
Depth below surface (m)	0.9	2.25	3.7	0.4	0.44
Water content δ§	1.317	1.164	1.388	1.275	1.354
U (μg/g) from ^{234}Th	4.45 ± 0.44	3.22 ± 0.40	4.40 ± 0.36	2.40 ± 0.22	3.39 ± 0.37
U (μg/g) from ^{226}Ra, ^{214}Pb, ^{214}Bi #	4.10 ± 0.14	2.38 ± 0.04	3.63 ± 0.23	2.02 ± 0.14	2.78 ± 0.24
U (μg/g) from ^{210}Pb	3.07 ± 0.53	3.42 ± 0.40	4.22 ± 0.32	2.19 ± 0.19	1.29 ± 0.40
Th (μg/g) from ^{208}Tl, ^{212}Pb, ^{228}Ac #	17.1 ± 0.6	12.1 ± 0.2	17.1 ± 0.2	8.86 ± 0.04	11.6 ± 0.5
K (%)	2.69 ± 0.13	2.35 ± 0.05	2.52 ± 0.05	1.92 ± 0.04	2.42 ± 0.14
A value	0.058 ± 0.005	0.066 ± 0.003	0.096 ± 0.012	0.072 ± 0.006	0.059 ± 0.003
Equivalent dose, D_e (Gy)	68.2 ± 2.4	50.8 ± 2.1	35.0 ± 2.5	21.8 ± 1.4	23.4 ± 0.7
Cosmic dose rate, dD_c/dt (Gy/k.y.) ††	0.1854 ± 0.0093	0.1759 ± 0.0088	0.1551 ± 0.0078	0.2409 ± 0.0120	0.1982 ± 0.0099
Dose rate, dD/dt (Gy/k.y.)	4.70 ± 0.41	4.58 ± 0.23	4.74 ± 0.48	3.24 ± 0.25	3.50 ± 0.33
OSL age (ka)	14.5 ± 1.5	11.1 ± 0.8	7.4 ± 0.9	6.7 ± 0.7	6.7 ± 0.7

†A radioactive disequilibrium was detected in these samples on a 1σ level, probably due to degassing of radon. The given dose rates dD/dt and OSL ages have been corrected for that. Without correction (i.e., using ^{226}Ra as representative equilibrium equivalent U-content), the ages would be WLL179: 14.1 ± 1.3 ka and WLL180: 6.3 ± 0.6 ka. As the correction had to be done under the assumption that the disequilibrium was in a steady state for the whole time after deposition, the corrected age represents only a better estimate than the equilibrium age and not necessarily the true age.

‡A minor radioactive disequilibrium was detected in this sample on a 2σ level, between ^{226}Ra and ^{210}Pb, probably due to influx of radon. Without correction, the dose rate for sample WLL360 would be 4.31 ± 0.23 Gy/k.y. and the OSL age would be 11.8 ± 0.8 ka.

§Ratio wet sample to dry sample weight. Errors were assumed to be 50% of (δ –1).

#U and Th content was calculated from the error weighted mean of the isotope equivalent contents.

††Contribution of cosmic radiation to the total dose rate was calculated as proposed by Prescott and Hutton (1994).

therefore interpreted as minimum ages for abandonment of the fluvial terraces by Saxton River. If the silt deposits are aeolian, blown from the active Saxton and Acheron River floodplains, then the OSL ages may significantly underestimate the tread abandonment age if there was a period of nondeposition between gravel abandonment and silt deposition. Extrapolating the OSL ages to the terrace tread and assuming a constant accumulation rate and an age of 0 ka for the ground surface would yield proxies for the maximum ages of the terraces. The samples from the trench (OSL-2 and OSL-3) were taken ~20 cm and 1 m above the gravel alluvium, respectively. These samples were dated to provide further age control for abandonment of T_1. Table 3 lists the results of our OSL dating; the age estimates for each terrace are discussed in the following paragraphs.

Abandonment of T_1 was dated by Knuepfer (1988) to 9.41 ± 1.57 ka, based on the thickness of pebble weathering rinds. Our sample OSL-1 from silt and fine sand collected 20 cm above the T_1 terrace gravels has yielded an age of 14.5 ± 1.5 ka, which is significantly older than the weathering rind age. Sample OSL-2, collected ~20 cm above the T_1 terrace gravels, in the Saxton trench, yielded an OSL age of 11.1 ± 0.8 ka. Both of these OSL ages indicate a late Pleistocene age for the terrace surface. Moreover, sample OSL-3, collected from a stratigraphically higher silt bed located ~1 m above the gravels in the Saxton trench, yielded a stratigraphically consistent age of 7.4 ± 0.91 ka. Finally the twelve ^{14}C age determinations from the Saxton trench on the T_1 surface are in correct stratigraphic order with respect to OSL-3 and each other. The oldest of the ^{14}C samples (sample 12, see Fig. DR-2, and Tables DR-1 and DR-2 [see footnote 1]) lies ~1 m above OSL-3 and has an age of ca. 5990–6290 cal. yr B.P. The T_1 terrace at Saxton River is now one of the best-dated fluvial terrace surfaces anywhere in New Zealand. Despite only surface clasts being selected for weathering rind measurement (Knuepfer, 1988), the large age difference between the OSL ages and the pebble weathering rind age is possibly, at least in part, the result of deflation of an original silt cover on the currently exposed pebbles. Pebbles presently exposed at the surface may have been previously buried by silt for an extended period of time predating their last exhumation, which would have delayed rind development on these once-buried clasts and resulted in an underestimation of the weathering age of the T_1 gravels. If the assumed fluvial origin of the silt that mantles T_1 is valid, then the OSL age of 14.5 ± 1.5 ka represents the best estimate of the time of abandonment of T_1. The OSL ages from the Saxton trench postdate deposition of the terrace gravels but also emphasize that Knuepfer's (1988) pebble weathering rind age of T_1 is likely to be an underestimation of the true age.

The two OSL samples of silt that immediately overlie the T_2 terrace gravels (OSL-4, OSL-5) yielded OSL ages of 6.7 ± 0.67 ka and 6.7 ± 0.74 ka, respectively. These results show a strong internal consistency and are also comparable to Knuepfer's pebble weathering rind age of 7.41 ± 1.1 ka. The OSL age of the T_2 terrace suggests that weathering rind calibrations return more accurate ages for younger (?Holocene) surfaces, consistent with the exponential decay pattern of weathering rind growth curves (Chinn, 1981). Given this observation, Knuepfer's (1988) weathering rind ages for the treads of the younger T_3–T_6 surfaces were adopted for slip-rate calculations in this study.

T_3 was not differentiated by Knuepfer (1988), and thus his pebble weathering rind age of 5.46 ± 0.77 ka for the T_4 terrace was used here as a minimum age for our T_3 terrace. The similar morphology of the two surfaces suggests that they are close in age. Abandonment of T_5 was dated by pebble weathering rind calibration at 4.0 ± 1.0 ka (Knuepfer, 1988). Two ages have been offered for T_6: a pebble weathering rind age of 2.0 ± 0.5 ka, which was attributed to deposition of the T_6 gravels (Knuepfer, 1988) and a ^{14}C age of 1.17 ± 0.11 ka from charcoal sampled from silty channel-fill and overbank sediments on the T_6 tread, which provides a minimum age for abandonment of T_6 (McCalpin, 1996a).

SLIP RATES

Slip rates calculated for each displaced terrace feature are quoted as a preferred value bracketed by minimum and maximum values (see Table 4). The preferred value was calculated by dividing the preferred offset estimate (as outlined already for each displacement; Table 1) by the mean

TABLE 4. SUMMARY OF TREAD AGE, RISER OFFSET, AND TREAD HEIGHT MEASUREMENTS, WITH OUR ESTIMATES OF THE LATERAL AND VERTICAL SLIP RATES OF THE AWATERE FAULT AND THE FLUVIAL INCISION RATE OF SAXTON RIVER

Terrace feature	Age (ka)	Horizontal offset (m)		Vertical offset (m)†	Tread height above river (m)	Lateral slip rate (mm/yr)		Vertical slip rate (mm/yr)†	Incision rate (mm/yr)
Hillslope		77	±15	2.6 ± 1.6		5.3	+1.8 −1.4	0.2 ± 0.1	
T_1 edge		81	±21			5.6	+2.3 −1.8		
T_1 tread	14.5 ± 1.5‡			3.0 ± 1.8	19.9 ± 2.0			0.2 ± 0.1	1.4 ± 0.1
T_1-T_2 riser		52	+6 −12			7.8	+2 −2.4		
T_2 tread	6.7 ± 0.7‡			1.9 ± 0.2	17.3 ± 1.7			0.3 ± 0.04	2.6 ± 0.1
T_2-T_3 riser		33	+3 −4			6.0	+1.6 −1.4		
T_3 tread	>5.46 ± 0.77§			0.7 ± 0.2	11.1 ± 1.1			0.1 ± 0.04	2.0 ± 0.2
T_3/T_4-T_5 riser		15	+0.5 −2.1			3.8	+1.3 −1.2		
T_4 tread	5.46 ± 0.77§				9.5 ± 1.0				1.7 ± 0.2
T_5 tread	4.0 ± 1.0§			−0.5 ± 0.2	4.7 ± 0.5			−0.1 ± 0.1	1.2 ± 0.3
T_5-T_6 riser		10	+0.5 −2			5.0	+2 −1.8		
T_6 tread	>1.17 ± 0.11#	6.3	±0.8	−0.4 ± 0.1	1.9 ± 0.2	5.4	+1.3 −1.1	−0.3 ± 0.1	0.9 ± 0.3

†A negative value indicates the sense of throw is up to the south.
‡Optically stimulated luminescence dating of fluvial silts (this study).
§Pebble weathering rind calibration (Knuepfer, 1992).
#^{14}C dating of carbonaceous overbank silts (McCalpin, 1996a).

age (as outlined in the previous section for each terrace thread; Table 4). The minimum slip rate was calculated by dividing the minimum offset by the maximum age, and the maximum slip rate was calculated using the maximum offset and minimum age. The slip rates calculated in this way are therefore asymmetric distributions around the preferred value. As mentioned earlier, we assumed that accrual of displacement of any given terrace riser was dated by the abandonment age of the terrace at its base. All the horizontal offsets and terrace ages at Saxton River are shown schematically in Figure 2B, and slip rates for each displacement are shown graphically in Figure 10. Brief explanations of each slip-rate estimate are given next.

The bedrock spur to the east of the Saxton River terraces has been offset by 77 ± 15 m. The OSL-based abandonment age of T_1 at 14.5 ± 1.5 ka provides a minimum age for accrual of this offset and yields a maximum average horizontal slip rate of 5.3 (+1.8, −1.4) mm/yr. The vertical offset of the hillslope of 2.6 ± 1.6 m yields a north-side-up slip rate of 0.2 ± 0.1 mm/yr. Offset of the T_1 back edge is likely to have started accruing at the same time as the terrace was abandoned, and therefore the slip rate derived from this offset and the T_1 age represents a more accurate slip rate than using the T_1 age to date the offset spur. The T_1 back edge has been offset by 81 ± 21 m, which yields a mean slip rate of 5.6 (+2.3, −1.8) mm/yr using the OSL abandonment age of T_1 of 14.5 ± 1.5 ka. The vertical offset of the T_1 tread of 3.0 ± 1.8 m yields a north-up slip rate of 0.2 ± 0.1 mm/yr.

Abandonment of T_2 at 6.7 ± 0.7 ka provides the estimated age for accrual of offset of the T_1-T_2 riser. When combined with the horizontal offset of 52 (+6, −12) m, this new OSL age yields a seemingly high slip rate of 7.8 (+2, −2.4) mm/yr. As mentioned already, measurement of the horizontal separation of the T_1-T_2 riser is complicated by the transtensional pull-apart at that site. This slip-rate value may therefore not be representative of the true rate, and

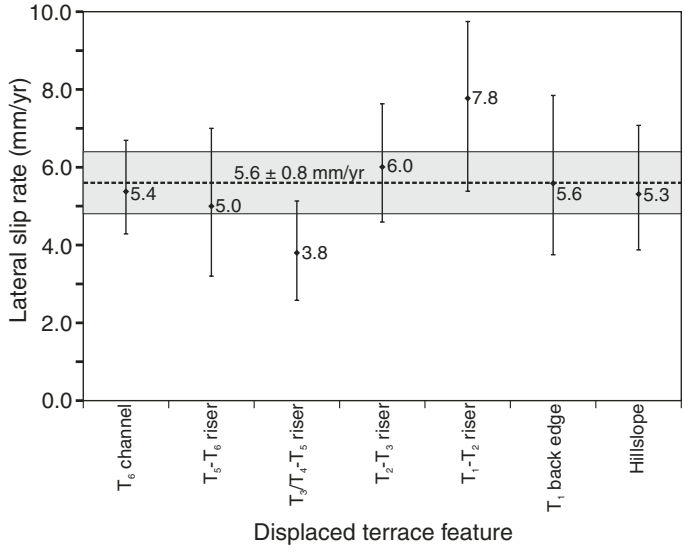

Figure 10. Plot of individual horizontal slip-rate estimates for each displaced terrace feature at Saxton River.

as such, should be viewed as a maximum rate. The vertical offset of the T_2 tread of 1.9 ± 0.2 m yields a vertical slip rate of 0.3 ± 0.04 mm/yr. This localized vertical slip rate must be viewed with caution, however, because of the transpressional pressure ridge uplifting the south side of the fault near the western edge of this tread.

Knuepfer's (1988) weathering rind age of the T_4 terrace (his "T_3" terrace) of 5.46 ± 0.77 ka is used here as a minimum age for offset of the T_2-T_3 riser. The lateral displacement of this riser of 33 (+3, –4) m results in a maximum horizontal slip rate of 6.0 (+1.6, –1.4) mm/yr, while vertical displacement of the T_3 terrace fragment (0.7 ± 0.2 m) yields a vertical slip rate of 0.1 ± 0.04 mm/yr, with the north side upthrown.

Knuepfer's (1988) weathering rind age of the T_5 terrace (his "T_4" terrace) of 4.0 ± 1.0 ka provides a maximum age for the lateral offset of the riser above this terrace of 15 (+0.5, –2.1) m. These data yield a minimum slip rate of 3.8 (+1.3, –1.2) mm/yr. The T_5 tread has been vertically offset by 0.5 ± 0.2 m, with the south side upthrown, which yields a vertical slip rate of 0.1 ± 0.1 mm/yr.

For lateral offset of the T_5-T_6 riser of 10 (+0.5, –2) m, Knuepfer's (1988) age of the T_6 terrace is 2.0 ± 0.5 ka, which yields a slip rate of 5.0 (+2.0, –1.8) mm/yr. McCalpin (1996a) ^{14}C-dated silt on top of T_6 to 1.17 ± 0.11 ka, which provides a minimum age for horizontal offset of the channel incised into the T_6 surface (6.3 ± 0.7 m) and vertical offset of the T_6 tread (0.4 ± 0.1 m, south side upthrown). These data yield a maximum lateral slip rate of 5.4 (+1.3, –1.1) mm/yr and a maximum vertical slip rate of 0.3 ± 0.1 mm/yr.

DISCUSSION

Temporal Variation in Rates of Late Quaternary Strike Slip on the Molesworth Section of the Awatere Fault

New dating of the Saxton River terraces and GPS-based surveying of terrace offsets allow us to refine estimates of late Quaternary slip rate for the Molesworth section of the Awatere fault. The mean slip rate since 14.5 ± 1.5 ka on the Awatere fault is calculated here to be (more or less) steady at 5.6 ± 0.8 mm/yr. The average slip rate of 5.6 mm/yr is derived from the numerical mean of the preferred slip-rate values (Fig. 10), and the symmetrical error of ±0.8 mm/yr is assigned from best-fit lines fitted to the displacement-age data as shown in Figure 11A. These slip rates fall within the inferred 95% uncertainty for each measured displacement and age estimate (see Fig. 11A). Offset of the T_1-T_2 riser (7.8 [+2, –2.4] mm/yr), suggests a mean slip rate that is slightly higher than 5.6 mm/yr, but within the uncertainties in slip measurement and dating, this data point is still within error of our suggested mean slip rate for the fault. Similarly, dextral slip of the riser above T_5 (3.8 [+1.3, –1.2] mm/yr), has a mean slip-rate estimate that is slightly lower than, but still within the error of the quoted value. As outlined already, the measurements of these two offsets are possibly less accurate than the rest of the terrace displacements. The simplest explanation, therefore, is that the slip rate on this part of the Awatere fault has been constant since the late Pleistocene.

The new slip-rate estimates differ significantly from the previous work of Knuepfer (1992), who suggested two intervals in the late Quaternary that differed significantly in their mean slip rate (Fig. 11B). Between 9.4–4 ka, he inferred that horizontal displacement accumulated at an average slip rate of 9.4 (+11.7, –4.1) mm/yr, whereas from 4 ka to the present, he inferred a much slower rate of horizontal slip at 3.8 (+2.5, –1.6) mm/yr. In contrast, our new data show no significant variation in the mean horizontal slip rates since abandonment of T_1 at ca. 15 ka. The lack of variation is predominantly due to our new OSL-based abandonment age of T_1, which is significantly older than Knuepfer's pebble weathering rind age. The large underestimation of the age of T_1 using weathering rind calibration, possibly due to a silt cover restricting rind growth on this terrace, overestimated the early Holocene slip rate. This required two separate line segments to fit the terrace offset data, ultimately resulting in a dramatic, but apparent, slowing of the horizontal slip rate after abandonment of T_5 at 4 ka.

Knuepfer (1992) also documented apparent decreases in lateral slip rate across most of the constituent faults of the Marlborough fault system during the Holocene, and interpreted these to be an expression of millennial-scale variability in the rates of plate boundary motions through northeast South Island. He argued that variations showed a ~5 k.y. periodicity, with reliable long-term motions only obtained by averaging incremental slip rates over 15–20 k.y. (Knuepfer, 1992). As argued already for the Saxton River terraces, dating late Quaternary geomorphic surfaces by pebble weathering rind calibration may result in the underestimation of the true age of at least the older, pre-Holocene

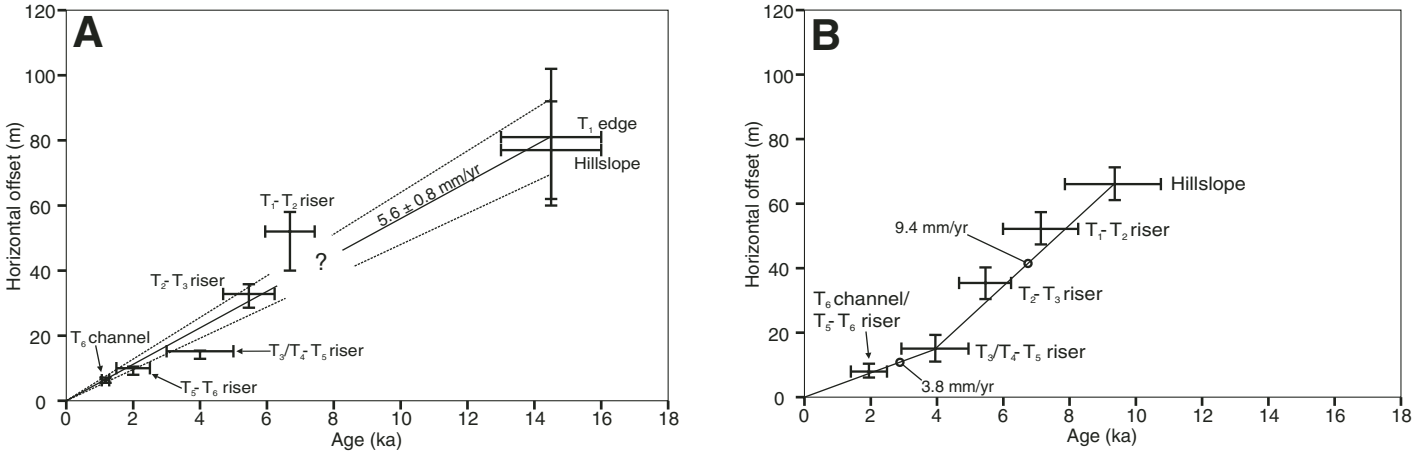

Figure 11. Plots of tread age and riser offset for each displaced terrace feature at Saxton River. (A) Data from this study, with refined ages of the two oldest terraces showing little or no variation in late Quaternary slip rate. Best-fit lines for offset and age data suggest a near-constant horizontal slip rate of 5.6 ± 0.8 mm/yr since ca. 14.5 ka. (B) Pebble weathering rind data as interpreted by Knuepfer (1992), showing an inferred decrease in lateral slip rate at ca. 4 ka.

terraces, resulting in a corresponding overestimation of Pleistocene slip rates calculated from the displacements of these surfaces. Our new abandonment ages for the Saxton River terraces suggest that horizontal slip rates of the Molesworth section of the Awatere fault have been approximately constant since 15 ka, with no evidence for millennial-scale variability in the rate of slip on that fault.

Slip rates calculated in this study for the Molesworth section of the Awatere fault show similarities, both in the rates of slip and the apparent lack of variability through the late Quaternary, to recent slip-rate estimates for the eastern section of the same fault. Little et al. (1998) and Benson et al. (2001) calculated slip rates from faulted alluvial terraces on the eastern section near Lake Jasper, documenting a near-uniform horizontal slip rate of 6 ± 2 mm/yr since ca. 20 ka. This is comparable to results from near Upcot Saddle on the eastern section, where strike-slip rates have been calculated at 5.6 ± 1.1 mm/yr (with a maximum rate of 8.2 ± 2.4 mm/yr) since the late Quaternary (Mason et al., 2004). Slip rates on the Molesworth section at Saxton River also show little variation through the late Quaternary, and the derived average rate of 5.6 ± 0.8 mm/yr is similar to the rates determined by Benson et al. (2001) and Mason et al. (2004) for the eastern section. New mapping of the fault junctions region between the eastern and Molesworth sections, and correlated timing of paleoearthquakes rupturing both sections across the junction provide the basis for the interpretation that the eastern and Molesworth sections of the Awatere fault may not be independent rupture segments, as previously inferred, but rather two geometric sections of a mechanically continuous strike-slip fault system (Mason et al., 2004). While not a priori evidence for such an hypothesis, the similarities and lack of variation of late Quaternary slip rates observed across the fault junction are consistent with the interpretation that the two fault sections are mechanically linked, with near-complete slip transfer between them.

Temporal (Holocene) Change in the Local Sense of Dip-Slip

Although the rate of strike-slip has not changed significantly during the late Quaternary on the Awatere fault, the sense of throw on that fault may not have been invariant during the same time period. At Saxton River, previous workers have noted a change in the sense of vertical offset during the Holocene, as evidenced by a switch from north-up offset of the T_1 and T_2 surfaces to south-up offset of the younger T_4 to T_6 surfaces (Knuepfer, 1992; McCalpin, 1996a). Similar changes in the sense of vertical offset have been observed on alluvial terraces at Grey River on the eastern section of the Awatere fault (Lensen, 1964b; Little et al., 1998) and elsewhere in the Marlborough fault system (e.g., Lensen, 1968; Knuepfer, 1992). A southeast-up sense of throw on the Awatere fault seems incongruous with respect to the long-term sense of dip-slip expressed by the long-wavelength topography (up to the northwest) along the Awatere fault (Little et al., 1998). Similarly, recent work on faulted alluvial terraces on the eastern section near Lake Jasper did not provide evidence for any reversal during the Holocene (Benson and Little, 2001). As seen in Table 1, the terraces at Saxton River record a late Holocene reversal in the sense of dip-slip that took place after abandonment of T_3 at 5.46 ± 0.77 ka (upthrown to the north) and before abandonment of T_6 at 1.17 ± 0.11 ka (upthrown to the south). The T_5-T_6 riser on the north side of the fault is 1.3 m higher than on the south side, implying that T_5 was upthrown to the north during occupation of T_6 (see Lensen, 1964a), and that south-up displacement since the throw reversal has removed any north-up offset of the tread. Based on this relationship, we infer that the throw reversal postdated abandonment of T_5 and could have occurred as recently as abandonment of T_6 at 2.0 ± 0.5 ka. Restoring the vertical offsets between the T_6 tread and the T_5 tread, however, suggests that the T_5 tread was upthrown ~0.5 m to the south at the time T_6 was abandoned, which is inconsistent with the north-up offset implied by the riser height difference. Therefore, the timing of the throw reversal at Saxton River cannot be constrained any narrower than post-T_3 (ca. 5.5 ka) and pre-T_6 (ca. 2 ka) abandonment.

The origins of similar throw reversals documented throughout the Marlborough fault system are contentious. Lensen (1968) noted a reversal in vertical offset at Branch River on the Wairau fault and concluded, without any geochronological data, that this occurred at the same time as a similar apparent reversal at Grey River on the Awatere fault (Lensen, 1964b). This apparent synchroneity has been interpreted in terms of a regional change in the horizontal direction of principal stress across the plate boundary zone in Marlborough (Lensen, 1973)—an unlikely scenario given the current spatial uniformity of maximum principal geodetic strain rates across northern South Island, New Zealand (Beavan and Haines, 2001), and their uniformly compressive disposition with respect to the Marlborough fault system. Knuepfer (1992) disregarded the regional stress change hypothesis, arguing that the throw reversals were not contemporaneous and suggesting that they were due to site-specific causes related to the local fault geometry.

Elastic modeling studies have suggested that changes in surface topography can perturb tectonic stress directions acting on subsurface planes (e.g., McTigue and Mei, 1981; Savage and Swolfs, 1986; Miller and Dunne, 1996). In particular, McTigue and Mei (1981) suggested that horizontal tensile stresses are induced in the near-surface beneath valley floors. At Saxton River, it is possible that rapid incision in the mid-Holocene (~15 m in the 3 k.y. time interval between 7 and 4 ka) may have perturbed the stress directions beneath the youngest terrace surfaces sufficiently to drive a reorientation of the near-surface fault dip and thus result in a change in the sense of dip-slip across the youngest terraces. This scenario is difficult to quantify, however, as it implies stress changes across a small area. Such a reorientation of the fault plane geometry is also not directly visible due to the active fault trace being obscured by the Saxton River floodplain. At a larger scale, however, the fault trace does change strike across the Saxton River valley (Fig. 1C). As noted earlier, a 5–10º change in the strike of the fault across the western edge of the T_2 tread has formed a 1–2-m-high, 60–80-m-long pressure ridge there. This restraining bend has uplifted the T_2 tread on the southern side of the fault, opposite to the north-side-up sense of throw of the T_1 and T_3 surfaces. While this pressure ridge is an exaggerated feature compared to vertical displacement of the adjacent treads, a similar reorientation of the fault dip may have been responsible for the switch to south-side-up throw of the youngest terraces. If such a hypothesis is true, then this suggests that feedbacks between fluvial incision (i.e., climate change), near-surface stresses, and fault geometry can cause short-term temporal changes in local dip-slip, without an equivalent change in the plate tectonically imposed strike-slip rate.

Relationship among Paleoseismicity, Terrace Displacements, and Size of Single-Event Surface Ruptures

The development of a detailed surface-rupture chronology from twelve ^{14}C ages and one OSL age from a paleoseismic trench excavated on the T_1 tread at Saxton River (ten events in less than 14.5 ± 1.5 k.y.; Mason et al., 2004) allows each dated terrace displacement to be attributed to a set of paleoseismically dated coseismic-slip increments. The fault trench logs and table of paleoearthquake ages are given in the data repository (Figs. DR-2, DR-5, and DR-6, and Table DR-3 [see footnote 1]). Using the chronology of terrace ages (Table 2), we divided the total displacement for any given terrace riser interval by the number of paleoseismically

resolved earthquakes during that interval to obtain a mean estimate of coseismic slip for that time period. Figures 12A and 12B compare the terrace offsets to the paleoseismic record, from which coseismic-slip increments can be derived. An important caveat for the interpretation of this diagram is to acknowledge the possibility of a bias in resolution of the earthquake record toward the younger part of the sequence, where a relatively sparse record has been preserved for events older than ca. 7 ka.

The ten earthquakes inferred from the trench excavations at Saxton River all occurred after deposition of the T_1 gravels at 14.5 ± 1.5 ka (Mason et al., 2004). The T_1 edge has been dextrally offset by 81 ± 21 m since this time, which yields a maximum average per event displacement of 8.1 ± 2.1 m over this interval. This is likely to be a significant overestimation, due to suspected sampling incompleteness and the few recognized rupture events in the trench older than 6 ka.

Total dextral displacement of the T_1-T_2 riser of 52 (+6, −12) m has accrued during at least the eight youngest surface ruptures, and possibly during nine events recognized by Mason et al. (2004). This suggests an average per event displacement of 5.9 ± 1.5 m. This is comparable in magnitude to the smallest (meter-scale) geomorphic displacements observed along both sections of the Awatere fault, which have been attributed to coseismic slip during the last surface-rupturing event (e.g., McCalpin, 1996a; Benson et al., 2001).

During the interval from T_3 abandonment to the present, there are seven, and possibly eight, recognized surface-rupturing events (Mason et al., 2004). Total displacement of the T_2-T_3 riser is 33 (+3, –4) m, resulting in an average coseismic displacement of 4.4 ± 0.8 m using these seven or eight events, which is similar to the result from the displacement of the T_1-T_2 riser.

The riser above the T_5 tread has been displaced by 15 (+0.5, –2.1) m. After abandonment of the T_5 tread, there were six or seven paleoearthquakes (Mason et al., 2004), which yields an average per event displacement of 2.2 ± 0.4 m. Similarly, total displacement of the T_5-T_6 riser of 10 (+0.5, –2.0) m accrued during three to five events, resulting in an average per event displacement of 2.55 ± 0.95 m. These are both significantly smaller than the displacements of 4–6 m inferred by McCalpin (1996a) to be single-event, coseismic offsets. Importantly, McCalpin (1996a) attributed displacement of the small channel incised into T_6 (measured in this study as 6.3 ± 0.8 m) to coseismic slip during only the most recent event, but the new paleoseismic data from Saxton River suggest that this offset accrued during the three or four surface ruptures that postdate the T_5-T_6 riser, implying a mean per event displacement of 1.9 ± 0.5 m. This seems to be an anomalously small value and suggests that McCalpin's ^{14}C age is an overestimation of the actual age of this channel. This scenario may be true if the material dated by McCalpin was detrital charcoal that was reworked into the silty overbank sediments that cap this terrace. Alternatively, this channel may have been continuously active during some of these four events, during which time it laterally trimmed the coseismic displacement of its banks.

Taken together, the paleoearthquake and terrace slip data record a history of variable per event coseismic slip on this part of the Awatere fault. Assuming that the earthquake history is complete back to ca. 6 ka, there has been an average of 4.4 ± 0.8 m of coseismic slip per event (using displacement of the T_2-T_3 riser) over 7–8 events. Between abandonment of the T_2-T_3 and T_5-T_6 risers, 18.5–28 m of lateral displacement accrued, resulting from at least three and possibly five surface-rupture events. This suggests an average single-event displacement during this time interval of 6.5 ± 2.8 m. After abandonment of the T_5-T_6 riser, the average displacement per event decreased to 2.55 ± 0.95 m.

In conjunction with the paleoseismic data of Mason et al. (2004), our terrace displacement data suggest that earthquake activity increased during the Holocene, with correspondingly reduced single-event offsets, despite a near-constant strike-slip rate. This relationship is consistent with a variable-slip model of earthquake behavior (e.g., Beanland and Berryman, 1991; McCalpin, 1996b) along this part of the Awatere fault rather than a characteristic earthquake model where coseismic displacements are relatively constant at any point along the fault (e.g., Schwartz and Coppersmith, 1984).

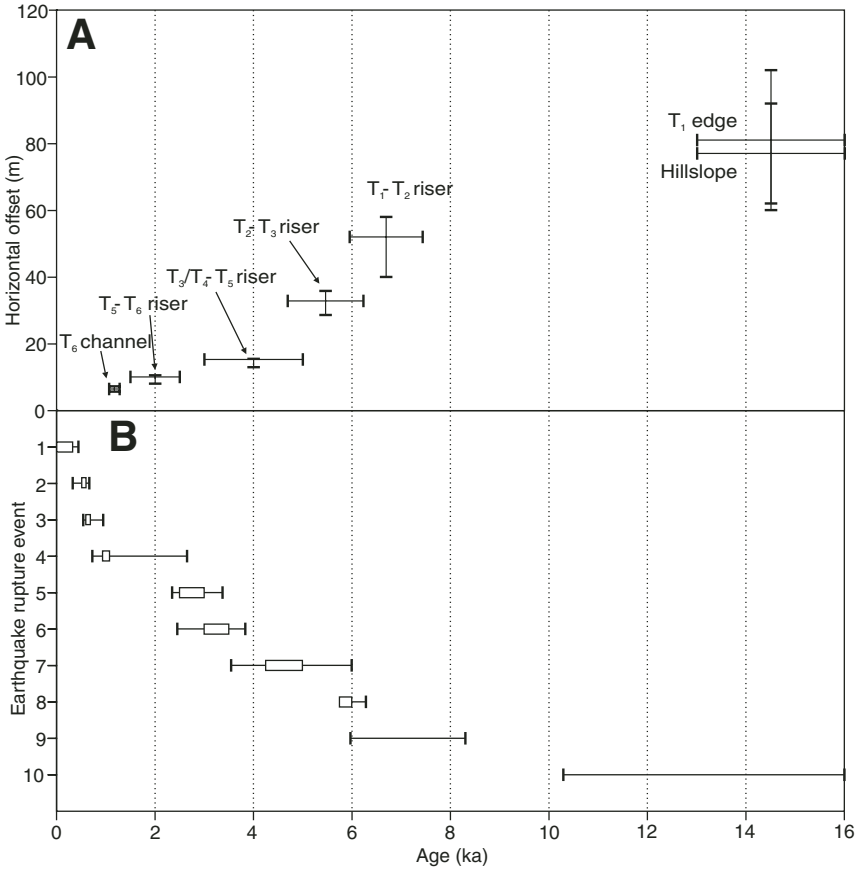

Figure 12. (A) Tread age and horizontal offset data from this study. (B) Bracketing and preferred ages of ten paleoearthquakes identified from paleoseismic study trench on the T_1 tread (Mason et al., 2004). Trench logs are shown in Figures DR4 to DR6 (see text footnote 1). The maximum permissible age ranges are provided by calibrated ages of radiocarbon samples that postdate and predate the inferred event. Preferred age ranges represent the most probable time of faulting based on the stratigraphic context of extrapolating event horizon ages between dated samples and assuming uniform sedimentation rates.

Late Quaternary Incision by Saxton River

The new OSL abandonment ages of T_1 and T_2 allow reconstruction of the incision history of Saxton River since the late Pleistocene. T_1 gravels were aggrading prior to ca. 15 ka, and possibly during the main late Otiran (last glacial) advance (ca. 18–20 ka; Suggate, 1990). Importantly, the abandonment age of T_1 suggests that aggradation by Saxton River continued into a period of regional increases in temperature and precipitation associated with deglaciation from 16.0 to 12.5 ka (Lambeck et al., 2002; Vandergoes and Fitzsimons, 2003). These increases in temperature and precipitation possibly removed any permanent snow cover from the catchment headwaters of Saxton River, and caused transportation of a previously "stored" fraction of ice-trapped detritus into the river, which was unable to transport the sediment beyond the transtensional basin at Isolated Flat. This process may have contributed to a marked increase in sediment flux that caused aggradation of the T_1 gravels. Continued increases in temperature and precipitation during the late Pleistocene, however, may have ultimately forced a switch from aggradation to incision, by further increasing the discharge and sediment transport capacity of the river at a time when sediment influx was being reduced as a result of reestablishment of vegetation cover within the catchment. The combination of these processes would trigger incision by Saxton River into the aggradation gravels, leaving an abandoned terrace tread (T_1).

A second, early Holocene glacial advance culminated at 9.2–9.5 ka (McCalpin, 1992a, 1992b), and T_2 was abandoned at 6.7 ± 0.7 ka. Therefore, both T_1 and T_2 were abandoned 2–3 k.y. after the culmination of glacial advances, rather than at the same time (cf. Berryman et al., 2000; Eden et al., 2001). The increases in temperature and precipitation that forced the glacial recessions may have released upstream repositories of glacial and periglacial sediment that had previously accumulated during the glacial advances. This allowed continued aggradation at a time when the transport capacity of the river might have been expected to increase. Following the transportation and aggradation of this previously stored detritus, continued increases in precipitation may have further increased the sediment transport capacity of Saxton River, resulting in abandonment and incision into the T_1 and T_2 treads.

The abandonment ages of the terraces and the heights of the treads above the contemporary floodplain of the river are shown in Figure 13, with a generalized, smooth curve fit to the data (cf. Bull and Knuepfer, 1987). Since abandonment of T_1 at 14.5 ± 1.5 ka, Saxton River has downcut 19.9 m below the T_1 tread into the underlying fluvial gravels. This suggests a mean incision rate of 1.4 ± 0.1 mm/yr in the late Quaternary. The incremental incision rates between dated terrace tread heights above the modern river, however, show three intervals in the late Quaternary over which fluvial incision has occurred at variable rates (Fig. 13). Downcutting from T_1 to T_2 occurred at a very slow rate of 0.33 ± 0.1 mm/yr. Such slow incision was possibly due to an early Holocene cooling in this area that facilitated glacial advances at Lake Tennyson and in the upper Wairau River valley (McCalpin, 1992a, 1992b), which may have restricted the supply of sediment to the river by re-covering the catchment headwaters with snow and ice.

Abandonment of T_2 in the mid-Holocene was followed by very rapid incision to T_5 (4.7 ± 1.3 mm/yr), suggesting very high stream power over this interval. Intensification of westerly winds in the mid- to late Holocene (e.g., Shulmeister, 1999) is one mechanism that could increase precipitation in the alpine inland Marlborough area at this time, which would have increased the transport capacity of Saxton River. Several terrace treads (T_3 to T_5) were cut and preserved since abandonment of T_2, suggesting brief pauses in downcutting during this period of rapid incision. These pauses may have been forced by short-term fluctuations in precipitation, temperature, and sediment availability, all of which would affect the transport capacity of the river (e.g., Bull and Knuepfer, 1987). In the latest Holocene, incision from T_5 to the present river level has occurred at a mean rate of 1.2 ± 0.3 mm/yr, similar to the long-term rate.

CONCLUSIONS

New OSL ages of cover sediments on faulted fluvial terraces at Saxton River, in combination with analysis of high-resolution GPS surveys of terrace displacements and previous age data, constrain progressive fault displacement of the terraces to a near-constant strike-slip rate of 5.6 ± 0.8 mm/yr since 14.5 ± 1.5 ka. Unlike previous studies, no evidence was found for a late Holocene decrease in the rate of strike slip on this fault or for variations in slip rate at the millennial scale.

Despite the constancy of the strike-slip rates, the sense of vertical slip varies from north-up displacement of the T_1 to T_4 surfaces to south-up displacement of the younger T_5 and T_6 surfaces. This throw reversal is constrained to between abandonment of T_3 (ca. 5.46 ± 0.77 ka) and abandonment of T_6 (1.17 ± 0.11 ka). The reversal was most likely not a regional widespread phenomenon, but instead may have been due to rapid fluvial incision in the early to mid-Holocene, which possibly increased horizontal tensile stresses beneath Saxton River and forced a local

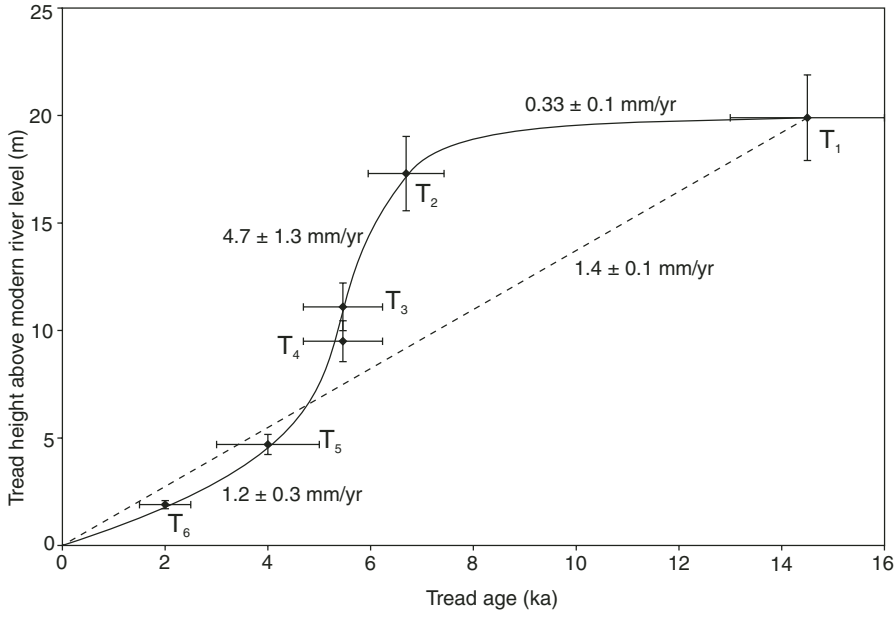

Figure 13. Plot of terrace tread ages against tread heights above Saxton River. This is used to estimate incremental fluvial incision rates between each terrace tread abandonment. These data show distinct periods over the late Quaternary in which incision rates have fluctuated. The age error bars are those outlined in Figure 12A; the tread height error bars are ±10%, which is an informal estimate of the measurement error.

change in the fault plane geometry beneath the youngest terraces sufficient to shift the sense of vertical offset. This hypothesis suggests that feedbacks between near-surface stresses, climate change, and fault geometry can induce a change in the kinematics of local dip-slip on a major strike-slip fault, without a corresponding change in the plate tectonically imposed strike-slip rate.

Comparisons between horizontal terrace riser displacements and a detailed surface rupture chronology of the Molesworth section yield a mean coseismic horizontal displacement of 4.4 ± 0.8 m over the eight most recent surface-rupture events. The youngest terrace riser displacements yield a mean coseismic displacement of <2.6 m, associated with an apparent late Holocene increase in earthquake frequency. This relationship is consistent with a variable-slip model of earthquake behavior along this part of the Awatere fault.

The new OSL age of abandonment of T_1 suggests that aggradation by Saxton River continued after the Last Glacial Maximum to 14.5 ± 1.5 ka, during a period of regional increases in temperature and precipitation. The increased temperature and precipitation possibly increased the flow capacity of Saxton River sufficiently to transport upstream repositories of glacial and periglacial sediment that had previously accumulated during the Last Glacial Maximum. Following a period of slow incision of 0.33 ± 0.1 mm/yr during occupation of the T_2 tread, Saxton River incised into the T_1 and T_2 alluvium. Fluvial incision rates by Saxton River in the late Quaternary are nonuniform, ranging from 0.33 ± 0.1 mm/yr in the late Pleistocene to 4.7 ± 1.3 mm/yr following abandonment of T_2. Rapid incision during the late Holocene suggests an increase in the transport capacity of Saxton River that was possibly forced by regional increases in precipitation and vegetation cover in the drainage catchment.

ACKNOWLEDGMENTS

This study was funded by the New Zealand Earthquake Commission and the Supplementary Research Fund of the Victoria University School of Earth Sciences. We thank Jim and Tracey Ward of Molesworth Station and Steve and Mary Satterthwaite of Muller Station for granting us access to their properties. An earlier draft of the manuscript was improved by the comments of J. Townend. Journal reviews by L. Owen, J. Lee, and J. McCalpin were very helpful in improving the manuscript. Field and technical assistance from T. Bear, N. Boyens, M. Hill, N. Hill, U. Rieser, D. Townsend, R. Wightman, and K. Wilson is also gratefully acknowledged.

REFERENCES CITED

Beavan, J., and Haines, J., 2001, Contemporary horizontal velocity and strain rate fields of the Pacific-Australian plate boundary zone through New Zealand: Journal of Geophysical Research, v. 106, no. B1, p. 741–770, doi: 10.1029/2000JB900302.

Benson, A.M., and Little, T.A., 2001, Temporal and spatial variability of Late Quaternary slip on the Awatere Fault: New Zealand Earthquake Commission Research Report 97/262, p. 2.1–2.40.

Benson, A.M., Little, T.A., Van Dissen, R.J., Hill, N., and Townsend, D.B., 2001, Late Quaternary paleoseismic history and surface rupture characteristics of the eastern Awatere strike-slip fault: Geological Society of America Bulletin, v. 113, p. 1079–1091, doi: 10.1130/0016-7606(2001)113<1079:LQPHAS>2.0.CO;2.

Berryman, K.R., and Beanland, S., 1991, Variation in fault behaviour in different tectonic provinces of New Zealand: Journal of Structural Geology, v. 13, p. 177–189, doi: 10.1016/0191-8141(91)90065-Q.

Berryman, K.R., Marden, M., Eden, D.N., Mazengarb, C., Ota, Y., and Moriya, I., 2000, Tectonic and paleoclimatic significance of Quaternary river terraces of the Waipaoa River, east coast, North Island, New Zealand: New Zealand Journal of Geology and Geophysics, v. 43, p. 229–245.

Bull, W.L., and Knuepfer, P.L.K., 1987, Adjustments by the Charwell River, New Zealand, to uplift and climatic changes: Geomorphology, v. 1, p. 15–32, doi: 10.1016/0169-555X(87)90004-3.

Carter, L., Lewis, K.B., and Davey, F., 1988, Faults in Cook Strait and their bearing on the structure of central New Zealand: New Zealand Journal of Geology and Geophysics, v. 31, p. 431–446.

Chinn, T.J.H., 1981, Use of rock weathering-rind thickness for Holocene absolute age-dating in New Zealand: Arctic and Alpine Research, v. 13, p. 33–45, doi: 10.2307/1550624.

De Mets, C., Gordon, R.G., Argus, D.F., and Stein, S., 1990, Current plate motions: Geophysical Journal International, v. 101, p. 425–478.

De Mets, C., Gordon, R.G., Argus, D.F., and Stein, S., 1994, Effect of recent revisions to the geomagnetic reversal time scale on estimates of current plate motions: Geophysical Research Letters, v. 21, p. 2191–2194, doi: 10.1029/94GL02118.

Eden, D.N., Palmer, A.S., Cronin, S.J., Marden, M., and Berryman, K.R., 2001, Dating the culmination of river aggradation at the end of the last glaciation using distal tephra compositions, eastern North Island, New Zealand: Geomorphology, v. 38, p. 133–151, doi: 10.1016/S0169-555X(00)00077-5.

Knuepfer, P.L.K., 1988, Estimating ages of late Quaternary stream terraces from analysis of weathering rinds and soils: Geological Society of America Bulletin, v. 100, p. 1224–1236, doi: 10.1130/0016-7606(1988)100<1224:EAOLQS>2.3.CO;2.

Knuepfer, P.L.K., 1992, Temporal variations in latest Quaternary slip across the Australian-Pacific plate boundary, north-eastern South Island, New Zealand: Tectonics, v. 11, p. 449–464.

Lambeck, K., Yokoyama, Y., and Purcell, T., 2002, Into and out of the Last Glacial Maximum: Sea-level change during oxygen isotope stages 3 and 2: Quaternary Science Reviews, v. 21, p. 343–360, doi: 10.1016/S0277-3791(01)00071-3.

Lensen, G.J., 1964a, The general case of progressive fault displacement of flights of degradational terraces: New Zealand Journal of Geology and Geophysics, v. 7, p. 864–870.

Lensen, G.J., 1964b, The faulted terrace sequence at the Grey River, Awatere Valley, South Island, New Zealand: New Zealand Journal of Geology and Geophysics, v. 7, p. 871–876.

Lensen, G.J., 1968, Analysis of progressive fault displacement during downcutting at the Branch River terraces, South Island, New Zealand: Geological Society of America Bulletin, v. 79, p. 545–556.

Lensen, G.J., 1973, Guidebook for excursion A10, *in* International Union for Quaternary Research Congress: Christchurch, New Zealand, 9th Congress, Field Trip Guide, 76 p.

Lewis, K.B., and Pettinga, J.R., 1993, The emerging, imbricate frontal wedge of the Hikurangi margin, *in* Ballance, P.F., ed., South Pacific Sedimentary Basins: Amsterdam, Elsevier Science, p. 225–250.

Little, T.A., and Roberts, A.P., 1997, Distribution and mechanism of Neogene to present-day vertical-axis rotations, Pacific-Australia plate boundary zone, South Island, New Zealand: Journal of Geophysical Research, v. 102, no. B9, p. 20,447–20,468, doi: 10.1029/97JB01279.

Little, T.A., Grapes, R.H., and Berger, G.W., 1998, Late Quaternary strike-slip on the eastern part of the Awatere fault, South Island, New Zealand: Geological Society of America Bulletin, v. 110, p. 127–148, doi: 10.1130/0016-7606(1998)110<0127:LQSSOT>2.3.CO;2.

Mason, D.P.M., Little, T.A., and Van Dissen, R.J., 2004, Influence of a fault-segment junction on the rupturing behaviour of the Awatere fault, New Zealand, and displacement-length measurement for the Marlborough earthquake rupture of 1848: New Zealand Earthquake Commission Research Report No. 01/442, 148 p.

McCalpin, J.P., 1992a, Glacial and post-glacial geology near Lake Tennyson, Clarence River, New Zealand: New Zealand Journal of Geology and Geophysics, v. 35, p. 201–210.

McCalpin, J.P., 1992b, Glacial geology of the upper Wairau Valley, Marlborough, New Zealand: New Zealand Journal of Geology and Geophysics, v. 35, p. 211–222.

McCalpin, J.P., 1996a, Tectonic geomorphology and Holocene paleoseismicity of the Molesworth section of the Awatere fault, South Island, New Zealand: New Zealand Journal of Geology and Geophysics, v. 39, p. 33–50.

McCalpin, J.P., ed., 1996b, Paleoseismology: San Diego, Academic Press, 583 p.

McSaveney, M.J., 1992, A manual for weathering-rind dating of grey sandstones of the Torlesse Supergroup, New Zealand: New Zealand Institute of Geological and Nuclear Sciences Science Report 92/4, 52 p.

McTigue, D.F., and Mei, C.C., 1981, Gravity-induced stresses near topography of small slope: Journal of Geophysical Research, v. 86, no. B10, p. 9268–8278.

Miall, A.D., 1992, Alluvial deposits, *in* Walker, R.G., and James, N.P., eds., Facies Models—Response to Sea Level Change: Ontario, Canada, Geological Association of Canada, 454 p.

Miller, D.J., and Dunne, T., 1996, Topographic perturbations of regional stresses and consequent bedrock fracturing: Journal of Geophysical Research, v. 101, no. B11, p. 25,523–25,536, doi: 10.1029/96JB02531.

Nicol, A., and Van Dissen, R.J., 2002, Up-dip partitioning of displacement components on the oblique-slip Clarence fault, New Zealand: Journal of Structural Geology, v. 24, p. 1521–1535, doi: 10.1016/S0191-8141(01)00141-9.

Prescott, J.R., and Hutton, J.T., 1994, Cosmic ray contributions to dose rates for luminescence and ESR dating: Large depths and long-term time variation: Radiation Measurements, v. 23, p. 497–500, doi: 10.1016/1350-4487(94)90086-8.

Savage, W.Z., and Swolfs, H.S., 1986, Tectonic and gravitational stress in long symmetric ridges and valleys: Journal of Geophysical Research, v. 91, no. B3, p. 3677–3685.

Schwartz, D.P., and Coppersmith, K.J., 1984, Fault behaviour and characteristic earthquakes: Examples from the Wasatch and San Andreas fault zones: Journal of Geophysical Research, v. 89, no. B7, p. 5681–5698.

Shulmeister, J., 1999, Australasian evidence for mid-Holocene climate change implies precessional control of Walker circulation in the Pacific: Quaternary International, v. 57–58, p. 81–91, doi: 10.1016/S1040-6182(98)00052-4.

Suggate, R.P., 1990, Late Pliocene and Quaternary glaciations of New Zealand: Quaternary Science Reviews, v. 9, p. 175–197, doi: 10.1016/0277-3791(90)90017-5.

Vandergoes, M.J., and Fitzsimons, S.J., 2003, The last glacial–interglacial transition (LGIT) in south Westland, New Zealand: Paleoecological insight into mid-latitude Southern Hemisphere climate change: Quaternary Science Reviews, v. 22, no. 14, p. 1461–1476, doi: 10.1016/S0277-3791(03)00074-X.

Walcott, R.I., 1998, Modes of oblique compression: Late Cenozoic tectonics of the South Island of New Zealand: Reviews of Geophysics, v. 36, no. 1, p. 1–26, doi: 10.1029/97RG03084.

Wellman, H.W., 1953, Data for the study of recent and late Pleistocene faulting in the South Island of New Zealand: New Zealand Journal of Science and Technology, v. 34, p. 270–288.

Manuscript Received 27 December 2005
Revised Manuscript Received 7 April 2006
Manuscript Accepted 6 May 2006

Printed in the USA